NEW CONSTRAINTS ON MARS PALEOCLIMATE FROM ORBITAL RADAR STUDIES OF POLAR AND MID-LATITUDE ICE DEPOSITS

J.W. Holt[1], R.J. Phillips[2]; S.R. Christian[1,3], B. Davis [4], I.B. Smith[1], T.C. Brothers[1], E. Quartini[1,5], K. Tanaka[6], and N. Putzig[2]. [1]University of Texas Institute for Geophysics, Jackson School of Geosciences, University of Texas, Austin, TX (jack@ig.utexas.edu); [2]Southwest Research Institute, Boulder, CO, [3]Department of Geology, Bryn Mawr College, Bryn Mawr, PA, [4]Colorado School of Mines, Golden, CO, [5]Dipartimento di Scienze della Terra e Geologico Ambientali, University of Bologna, Bologna, Italy, [6]U.S. Geological Survey, Flagstaff, AZ

Introduction: The distribution and time variability of ice on Mars provides important constraints on atmospheric processes. Until the advent of orbital radar sounding at Mars, our understanding of ice has been based on observations limited to the surface and near-surface (tens of centimeters depth). Studies of outcrops in the polar layered deposits using optical and high-resolution morphological methods have attempted to assess the character and continuity of exposed layers in order to quantify spatial heterogeneity (both vertical and horizontal) and have attempted to link compositional layering to climate with the primary objective of correlating observed patterns with orbital forcing parameters (reviewed by [1]). Likewise, geological evidence in the middle and low latitudes has been found to support the hypothesis that large quantities of ice have been transferred between the poles and lower latitudes [2].

Orbital radar has provided new insights into icy deposits by probing the subsurface to depths of kilometers and detecting internal properties [3-5]. We have found that internal stratigraphy of the north polar layered deposits (NPLD) preserves a rich record of deposition, erosion and transport exhibiting strong evidence of polar landscape evolution dominated by atmospheric processes rather than englacial flow or sub-ice processes [6,7].

Although internal radar stratigraphy in the south polar layered deposits (SPLD) is more challenging, we have found evidence for large quantities of sequestered CO2 ice just below the surface, implying the potential for significant, geologically recent variability in the CO2 content of the atmosphere and total atmospheric pressure.

In the southern mid latitudes, we have found evidence for multiple glaciation events leading to the accumulation of a large glacial complex in the eastern Hellas region. All of these results provide new, quantifiable constraints (both volumetric and spatial) on the evolution of volatiles previously unavailable to climate modelers.

Methods: The Shallow Radar (SHARAD) instrument on Mars Reconnaissance Orbiter (MRO) is a chirped radar operating at a 20 MHz center frequency (15 meters free-space wavelength) [8]. Its 10 MHz bandwidth yields a theoretical vertical resolution of ~ 9 m in water ice. Horizontal resolution is 0.3 – 1 km along-track and 3 – 6 km across track.

Data from SHARAD passes were processed with a focused synthetic aperture radar (SAR) technique in order to reduce along-track surface clutter and resolve reflectors with relatively steep slopes. Radar reflectors were traced using seismic analysis interpretation tools on hundreds of intersecting lines. This allows the quantitative extraction of radar reflector positions in time and tracking of reflectors across multiple lines.

Radar stratigraphy of the NPLD: Many radar reflectors exist, and most extend across the entire NPLD [5,9]. The presence of stratigraphic uncon-

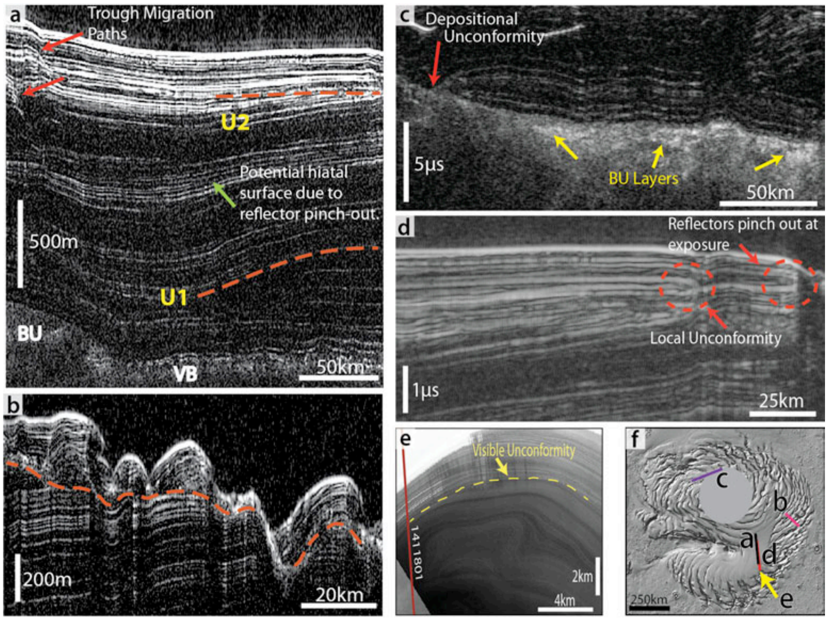

__Figure 1.__ Stratigraphic complexity in the NPLD. __(a)__ SHARAD observation 5297_01 showing deep unconformities (red dashed lines) and significant thickness variations between reflectors. Red arrows indicate structures related to trough migration [Smith and Holt, 2010]. VB = Vastitas Borealis Fm. __(b)__ Observation 7616_02 showing an extensive unconformity near the margin of PB. __(c)__ Multiple reflectors near base of NPLD that pinch out against the BU, defining an outer edge of accumulation. __(d)__ Smaller, possibly local, unconformities near outer margin of PB. __(e)__ CTX imagery showing visible layer unconformity near SHARAD observation (d). Location map for all data in lower right. (1 μs = ~168 m vertical thickness in ice.)

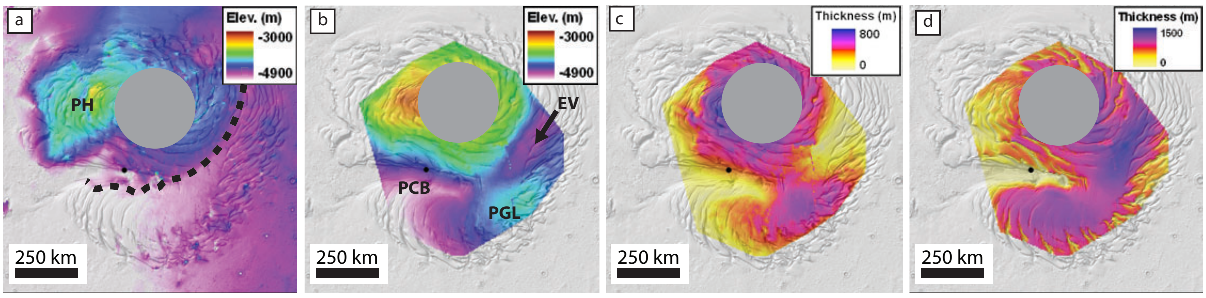

Figure 2. *Examples of paleosurfaces and net accumulation maps that can be derived from SHARAD analysis. For all maps shown here, the present-day surface is included as semi-transparent, shaded-relief greyscale overlay. (a) Base of NPLD, merged with surrounding MOLA elevations to show context and continuity. Buried boundary of basal unit (BU) shown as dashed line, as determined from our mapping. PH = paleo high. (b) Surface elevation of unconformity U1 (Fig. 1a) and its stratigraphic equivalent elsewhere. PGL = paleo Gemina Lingula; PCB = paleo Chasma Boreale; EV = eastern valley. (c) Net accumulation thickness prior to the U1 surface. (d) Net accumulation thickness between U1 and present-day surface. Note change in total range of color scale between (c) and (d). Adapted from [6]*

formities can be used to identify significant changes in accumulation (e.g., depositional hiatuses accompanied by erosion). This is demonstrated in Fig. 1 where several types of unconformities are identified. The existence of many unconformities points at various stratigraphic levels points to a fundamental problem with attempts to correlate sequences of layers with orbital forcing parameters, since a continuous layer sequence appears to be unlikely.

Furthermore, multiple lines of evidence provided by radar sounding, including the presence of deep, angular unconformities and comparisons of internal layer morphology with those predicted by a flow model [10], indicate that ice flow has not significantly influenced NPLD stratigraphy. In addition to the implications for the history of polar temperatures, this allows for the interpretation of radar reflectors as representing virtually undeformed paleosurfaces, a key component of our later analyses.

We first mapped the base of the NPLD using hundreds of SHARAD orbits, as in [6, 9]. We then mapped the radar reflectors that immediately overly U1 across Planum Boreum, including where they are conformable to the underlying layers within the main lobe. Converting time delays to absolute elevation using the surface echo as a reference and the velocity radar in water ice [11], we constructed elevation maps of the base and the paleosurface that existed at the end of the hiatus represented by the U1 unconformity (Figs. 2a and 2b, respectively). By differencing the three surfaces (base, mid-level and present surface), we can map net accumulation before and after the U1 erosional event (Figs. 2c and 2d).

Surface evolution of the NPLD: Our maps show that in spite of initial deposition being widespread and uniform (indicated by near-uniform, subhorizontal radar layering below U1; Fig. 2a), the net accumulation pattern that includes erosion during the U1 hiatus was not uniform. An elongate, nearly isolated lobe of PLD was formed at this time, adjacent to the polar high created by the BU and early NPLD deposition. This "proto Gemina Lingula" (PGL; Fig. 2b) formed the southern margin of a "proto Chasma Boreale" (PCB; Fig. 2b) which was matched by a second chasma that is no longer evident on the Planum Boreum surface (EV, for Eastern Valley; Fig. 2b).

Topographic/atmospheric feedbacks: We propose that high topography and steep slopes resulting from the BU surface produced katabatic winds that eroded the earliest NPLD deposits to form PGL, PCB, and EV during a depositional hiatus. During subsequent deposition (Fig. 2d), EV was completely filled in while PCB was not. This is the strongest evidence for large-scale, non-uniform deposition within the NPLD. We suggest that this was due to the influence of topography affecting accumulation patterns in that climatic regime. The presence of PGL clearly played an important role in today's topography, as layers above U1 drape the PGL surface (Fig. 2) and largely maintain its shape.

New mapping is underway to characterize detailed accumulation patterns in finer detail and map erosional surfaces throughout the NPLD. This will provide a sequence of depositional and erosional events. This sequence could then perhaps be linked to quasi-periodic global climate change driven by orbital parameters, as has been attempted for layer sequences.

Sequestered CO_2 in the SPLD: While well-organized sets of radar reflectors are ubiquitous in the NPLD, those in the SPLD are limited to specific regions, and it is difficult to map SPLD-wide radar stratigraphy. What is evident, however, are four regional reflection-free zones (RFZ) distinguished qualitatively by their radar characteristics. They are up to a kilometer in thickness and extend downward from near the surface.

One such zone (RFZ_3) occurs beneath the South Polar Residual Cap (SPRC), which is composed of ~5 m of solid CO_2 underlying an apparently thin layer of water ice. Using a correlation technique on reflectors below this zone, we inverted for the real permittivity, ε', on each of 41 usable SHARAD orbits over RFZ_3. The results were mean values of $\varepsilon' = 2.0$ or 2.1, with a σ of 0.2.

An additional technique based on the "smoothest" solution to layer continuity gave similar results.

These values are exceptionally close to the laboratory-measured permittivity value of bulk CO_2 ice [12] and distant from the bulk water ice value (ε' = 3.15) and the pure CO_2 clathrate value (estimated ε' = 2.85). An alternative hypothesis is that the RFZ_3 material is porous water ice, but this can be strongly discounted based on theoretical and empirical models of ε' of porous water ice vs. thickness. By the same arguments, the proposed CO_2 material also cannot be very porous, and ε' should be close to the bulk value, which is corroborated by other observations.

With the permittivity estimates, radar time delays were converted to depth, and for RFZ_3 a mean thickness of 210-220 m and a volume of 4,200-4,400 km^3 result. This is unlikely to be the entire volume because MRO's orbital inclination precludes SHARAD sounding poleward of ~87°S, where RFZ_3 appears to extend.

We do find a very good spatial correlation of RFZ_3 with the stratigraphic unit (named "Aa_3") immediately beneath the SPRC [13] and use this geologic unit as a basis for extrapolation, yielding a volume estimate range of 9,500 to 12,500 km^3. For comparison, the CO2 in the SPRC is estimated to be < 380 km^3 [14]. The equivalent atmospheric pressure of the extrapolated RFZ_3 volume is 4-5 mbar, competing in magnitude with the current atmospheric pressure of 6-7 mbar. The other three reflection-free zones may also contain a component of CO_2, but the reflector geometry is not favorable for estimating permittivity.

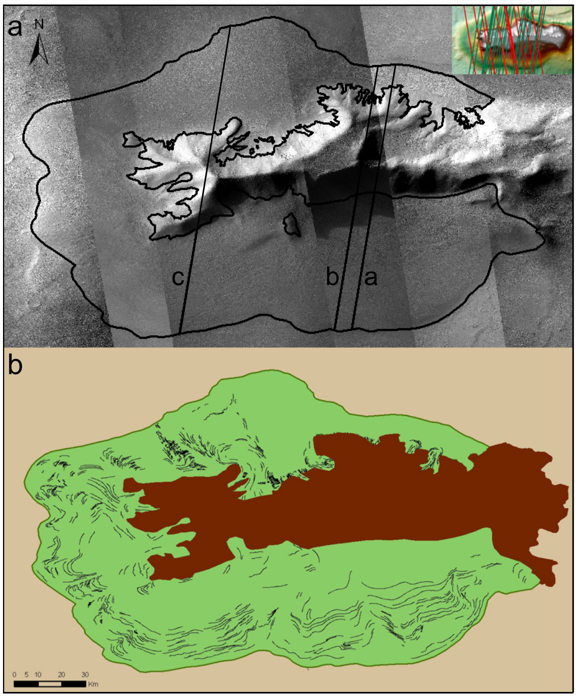

Figure 3. *Lobate debris apron (LDA) complex east of the Hellas Basin in the southern hemisphere, found to contain massive glacial ice, up to 800 m thick [15].* ***(a)*** *outline of LDA based on mapping in CTX imagery draped on MOLA-based topography. SHARAD tracks for Fig. 4 indicated.* ***(b)*** *Surface lineations indicating past flow, sketched onto geologic map (green is the LDA, brown is the massif). Separate flow lobes can be delineated in this way.*

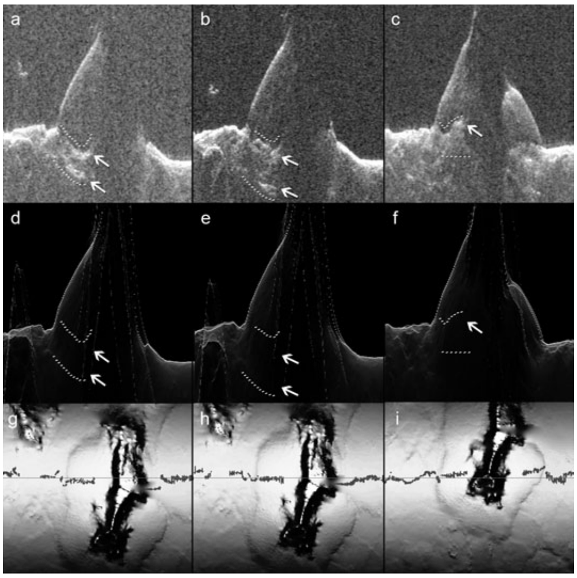

Figure 4. *Examples of radar detections of an older unit below main LDA ice deposit, providing evidence for an older glaciation.* ***(a-c)*** *SHARAD data with subsurface reflections from top and bottom of lower unit indicated with arrows (see Fig. 3 for locations).* ***(d-f)*** *Surface clutter simulations. Where an echo in the data does not exist in the simulation, the echo can arise from a subsurface reflector.* ***(g-i)*** *Simulated echo brightness maps and points of primary surface echo location. Ground track of MRO shown as horizontal line. The two simulations confirm the subsurface source of echoes and their geographical locations. Note significant variability between the lobe crossed by (a) and (b) compared to (c).*

Mid-latitude glaciations: SHARAD confirmed the previously hypothesized existence of massive glacial ice in the middle latitudes of Mars, within features known as "lobate debris aprons" (LDAs) that exhibit flow features on the surface, although the surface is composed of rocky debris and dust, similar to surrounding areas [15,16]. In contrast to polar ice, these LDAs lacked initial evidence for a layered internal structure detectable by the radar. The lack of layering supported the idea that these were largely formed in a single, widespread event. Questions remain regarding relative timing between different regions and whether the glaciers are the remnant of a larger ice sheet, or represent the final stage of coalescing, alpine-style glaciers. The formation mechanism of the protective surface layer is of course still a major unknown.

We have further examined a large LDA complex in the eastern Hellas region using many SHARAD observations. Through this analysis we have found evidence for an older glacial event represented by additional radar reflections near the base of the deposit; furthermore, significant lateral variability within the older unit indicates that it could have been formed through the alpine-style glaciation process, while the relatively more recent unit exhibits much less lateral variation. This could imply different climatic regimes leading to the two events.

Conclusions: Orbital radar studies using SHARAD have revealed quantifiable patterns of accumulation, large-scale erosional events, and compositional variations in the polar deposits of Mars including a large, previously-undetected reservoir of CO_2 ice. Studies of mid-latitude glacial deposits indicate the preservation of ice from multiple glaciations that resulted from the transfer of ice from the polar regions to lower latitudes.

All of these observations provide important and entirely new constraints for the modeling of past climate in order understand the long-term evolution of volatiles on Mars.

Acknowledgements: This work was supported by the MRO project through a JPL contract to JWH, and NASA grant NAG5-12693 to JWH. We thank P. Choudhary for assistance with data analysis.

References: [1] Fishbaugh, K.E. et al. (2008) *Icarus*, 196, 305–317. [2] Head, J.W., et al., (2003) *Nature* 426, 797-802. [3] Picardi et al. (2005) *Science* 310(5756), 1925-1928. [4] Seu et al. (2007) *Science* 317, 1715-1718. [5] Phillips et al. (2008) *Science*, 320, 1182-1185. [6] Holt, J.W. et al. (2010), *Nature* 465, 446-449 [7] Smith, I.B. & Holt, J.W. (2010) *Nature* 465, 450-453. [8] Seu, R. et al. (2007) *Jnl. Geoph. Res.*, 112. [9] Putzig N. E. et al. (2009) *Icarus*, 204, 443. [10] Karlsson et al. (2010) *LPSC 41*, Abs. 1781. [11] Grima C. et al., (2009) *Geoph. Res. Lett.*, 36, L03203. [12] Pettinelli et al. (2003) *Jnl. Geoph. Res*. 108, 8029. [13] Kolb et al. (2006) *LPSC 37*, Abs. 2408. [14] Thomas et al. (2009) *Icarus* 203, 352. [15] Holt et al. (2008) *Science* 322, 1235. [16] Plaut et al. (2009) *Geoph. Res. Lett.*, 36, L02203.